



HAL
open science

Ranking of epistemic uncertainties in scenario-based seismic risk evaluations

Pierre Gehl, Thomas Ulrich, Jeremy Rohmer, Caterina Negulescu, Ariane Ducellier, John Douglas

► **To cite this version:**

Pierre Gehl, Thomas Ulrich, Jeremy Rohmer, Caterina Negulescu, Ariane Ducellier, et al.. Ranking of epistemic uncertainties in scenario-based seismic risk evaluations. 11th International Conference on Structural Safety & Reliability: ICOSSAR 2013, Jun 2013, New-York, United States. pp.1-7. hal-00821362

HAL Id: hal-00821362

<https://brgm.hal.science/hal-00821362>

Submitted on 8 Jun 2013

HAL is a multi-disciplinary open access archive for the deposit and dissemination of scientific research documents, whether they are published or not. The documents may come from teaching and research institutions in France or abroad, or from public or private research centers.

L'archive ouverte pluridisciplinaire **HAL**, est destinée au dépôt et à la diffusion de documents scientifiques de niveau recherche, publiés ou non, émanant des établissements d'enseignement et de recherche français ou étrangers, des laboratoires publics ou privés.

Ranking of epistemic uncertainties in scenario-based seismic risk evaluations

P. Gehl, T. Ulrich, J. Rohmer, C. Negulescu, A. Ducellier & J. Douglas

*Risks and Prevention Division — Seismic and Volcanic Risks Unit
BRGM, Orléans, France*

ABSTRACT: In the scope of a scenario-based risk analysis, this study aims to quantify and rank various types of epistemic uncertainties that enter into the derivation of fragility functions for common buildings. Using a numerical model of a test structure (a reinforced concrete five-story building with infill panels on the first two floors), a first type of uncertainty is introduced, consisting of the mechanical properties of the materials (i.e. Young's modulus and compressive strength for concrete, and Young's modulus and yield strength for steel). The area of longitudinal reinforcement is also modified in the model, to generate various damage mechanisms for the same structure, depending on which floor first experiences failure. Finally, another source of epistemic uncertainty is studied, by comparing different types of fragility models: fragility curves derived from dynamic analyses and fragility functions generated from a capacity spectrum approach (i.e. use of a set of natural response spectra to identify a series of performance points from the capacity curve).

To this end, a ranking of the importance of different sources of uncertainty in the vulnerability analysis (i.e. mechanical properties, structural models and fragility models) is conducted by computing, for each uncertainty source, the Sobol' indices (i.e. the main effects and total effects of each source of uncertainty). This variance-based sensitivity technique presents the appealing features of both exploring the influence of input parameters over their whole range of variation and fully accounting for possible interactions between them. Nevertheless, addressing the issue of sensitivity to model uncertainty implies paying special attention to the appropriate treatment of different types of input parameters, i.e. continuous for mechanical properties or categorical in the case of fragility models. This is achieved by relying on recent advances in functional variance decomposition. For all these types of models, a uncertainty analysis in terms of the predicted number of damage buildings is carried out for a series of hypothetical scenarios.

1 INTRODUCTION

While best practices for probabilistic seismic demand analysis for single sites (i.e. specific elements at risk such as bridges or high-rise buildings) have been rigorously developed in the past decade, the application of earthquake risk (and loss) scenarios at the scale of a municipality or a region have received less attention in the recent literature. In these scenarios expected damage given the occurrence of one of a handful of earthquakes is estimated through fragility functions relating the ground motion to the level of damage. However, due to the presence of various building types at the scale of an urban area, these buildings are often assigned to specific typologies and appropriate fragility curves selected from the literature, which could lead to a large variation in the fragility models used. This issue has been highlighted by Crowley et al. (2011), who have compared disparate models, following a review of existing fragility functions

for reinforced concrete (RC) structures. In this study the focus is, therefore, on the implications of different sources of epistemic uncertainties (the structural properties, the structural models and the procedure for the derivation of fragility curves) on the parameters of fragility functions that could be used in a given scenario.

The effects of strong-motion variability and random structural parameters on fragility curves for an RC building have been studied for instance by Kwon and Elnashai (2007), who concluded that the effect of strong-motion variability was the largest. Zentner (2011) has also quantified, through the computation of Sobol' indices, the influence of various uncertainties (namely: seismic demand, mechanical parameters and damping ratio) in the case of numerical dynamic analyses applied to a single RC structure, thereby showing the predominant role of the variability of seismic demand. The propagation of uncertainties related to mechanical parameters, has also been studied

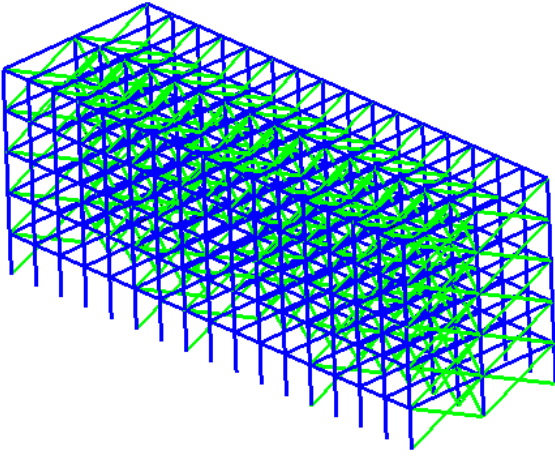


Figure 1: 3D view of the finite element model of the test structure.

by Pagnini et al. (2011) in the case of the estimation of capacity curves and performance points for masonry buildings. They found, in this case, that the uncertainties in the building stock parameters may be neglected with respect to model errors or seismic demand. Finally, the importance of various modeling assumptions (slab modeling, infill panels or mass modeling) on the resulting capacity curves has been stressed by Sousa et al. (2012) for several RC structures.

The present study will therefore focus on some epistemic uncertainties, in terms of mechanical properties or model variants, that are introduced in the vulnerability assessment for both types of analyses (i.e. based on capacity curves or on dynamic time-history simulations). These sources of uncertainty are then ranked thanks to the computation of Sobol' indices and, finally, the overall impact of the dispersion in the fragility curves is presented with respect to the proportion of damaged or collapsed buildings for a few hypothetical scenarios.

2 TEST STRUCTURE

Fragility models are developed and hypothetical risk scenarios are evaluated for a test structural type. The selected structure has been previously modeled and studied by Negulescu et al. (2013). It is a five-story reinforced concrete structure (regular in plan and elevation) that can be considered as 'pre-code' since it is designed against gravity loads only. The building has a width of 14.5 m in the transverse direction and a length of 45 m in the longitudinal direction. It is 18.6 m high and it contains some interior infill walls for partitioning. A three-dimensional finite element model of the structure has been built with the OpenSees platform. Beams and columns components are used to model the frames, and truss elements are used to represent the infill walls (Figure 1).

Table 1 lists the mechanical properties for concrete and steel that have been selected, based on some assumptions and the formulation of strain limits for an uniaxial Kent-Scott-Park model (Kent and Park 1971) with tensile strength and linear tension softening.

Table 1: Mechanical properties for the constitutive models of concrete and steel.

Parameter	Value	
Concrete compressive strength	f_c	25 MPa
Concrete strain at compressive strength	ϵ_{c0}	0.004
Concrete crushing strength	f_{cu}	4 MPa
Concrete strain at crushing strength	ϵ_{cu}	0.008
Steel yield strength	f_y	450 MPa
Steel elastic Young modulus	E_0	200 GPa
Steel strain hardening ratio	b	0.005

A modal analysis gives the first vibration mode at a period $T_1 = 0.33$ s and the second one along the longitudinal direction at $T_2 = 0.12$ s. These findings are in good agreement with the modes estimated from ambient vibration measurements on the building (Negulescu et al. 2013), thus verifying the accuracy of the structural model in the elastic range. Here, the inter-story drift ratio (i.e. the horizontal displacement between two stories per unit of height) has been chosen as the engineering demand parameter representing the structural damage. Based on a static pushover analysis (see Figure 2) and on the results of the incremental dynamic analysis performed by Negulescu et al. (2013), the yield drift is set as $d_y = 0.20\%$ and the ultimate drift is estimated to be equal to $d_u = 2.68\%$. Finally, using the relation between displacement limits and EMS-98 damage states (Grünthal 1998) proposed by the Risk-UE project (Milutinovic & Trendafiloski 2003), drift limits are estimated and can be used to identify the damage states of the studied structure. For simplicity Crowley et al. (2011, Gehl et al. (2013), we consider only two damage levels out of the five available in the EMS-98 scale. The first damage state, designed as 'yield' or 'slight', corresponds to the merger of EMS-98 damage levels D1 to D3; the corresponding drift threshold is 0.14%, based on the values of d_y and d_u . The second damage state corresponds to a near-collapse/collapse configuration and it includes both D4 and D5 damage levels; it is reached when the inter-story drift attains 0.68%.

3 MODELLING OF EPISTEMIC UNCERTAINTIES

This section is devoted to the definition of the sources of uncertainties that intervene in the fragility functions derivation.

3.1 Distribution of mechanical properties

First, a small set of mechanical parameters for the steel and concrete materials are assigned a probabilistic distribution to account for local variations and differences in the quality of the materials used during the construction. Several past studies (Zentner 2011, Jalayer et al. 2010, Rota et al. 2010, among others) have proposed variation ranges for different types of materials. Based on the existing literature and the Eurocode guidelines (Eurocode 2 2005) as well as

Table 2: Probability distributions of mechanical properties for concrete and steel.

Parameter		Probabilistic model	Coefficient of variator
Concrete compressive strength	f_c	lognormal	20%
Concrete initial Young's modulus	E_{c0}	lognormal	20%
Steel yield strength	f_y	lognormal	10%
Steel elastic Young's modulus	E_{s0}	lognormal	10%

FEMA recommendations (ASCE 2007), some average variations ranges are proposed for four mechanical properties (see Table 2).

Lower and upper bounds are also assigned to these mechanical properties to prevent the sampling of unrealistic values. This procedure is equivalent to defining an truncated lognormal distribution, where the bounds are set at ± 2 standard deviations. Finally, it should be noted that the variation in the steel and concrete parameters is only introduced in the RC-frame elements, and the characteristics of the trusses that are used to model the infill walls remain unchanged.

3.2 Types of structural models

The influence of the occurrence of different damage mechanisms is also studied, by altering the deformation pattern along the building height. To this end, the value of the section of steel reinforcements is altered in the first two stories of the building. Thanks to this procedure, three variants of structural models are generated, each one of them inducing damage concentration at different stories:

1. steel reinforcements are uniform in the first two stories and the largest deformations occur in the first story;
2. section of reinforcements is doubled in the first story and increased by 50% in the second story, leading to an increased participation of the first two stories to the lateral resistance and larger deformations in the third story; and
3. only the reinforcement section in the first story is doubled and the damage results in larger deformations in the second story.

These changes, therefore, alter the behavior of the structure in the non-linear range and enable selection of the stories that are likely to be damaged the most. This may have a non-negligible impact when static or dynamic analyses are performed during the derivation of fragility functions. The pushover curves for the three models are represented in Figure 2. The peaks at the beginning of the curves represent the stiff stories that undergo an early strength degradation due to the failure of infill walls. When comparing the three curves, the difference in the levels of displacement where the peaks occur results directly from which story is affected first by the incremental horizontal loading. In the case of model 1, the infill in the first

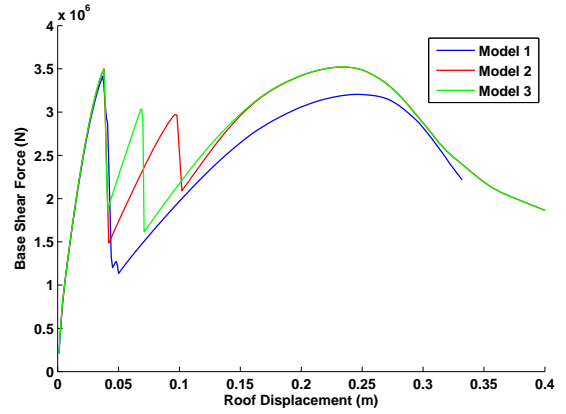


Figure 2: Pushover curves of the three structural models, using the mechanical properties from Table 1.

story is the first to endure failure (i.e. the single peak on the blue line) and the global response of the building is almost solely conditioned by the behavior of the first story. In the case of models 2 and 3, a second peak (i.e. on the red and green lines) represents the failure of the second or third stories, due to the improved resistance of the first story of the RC frame, which compels the next stories to contribute to the deformation distribution. However, it can be noted that the initial stiffness of the building remains unchanged, as well as the global behavior in the near-collapse range.

3.3 Types of fragility models

Finally, the last source of uncertainty that is considered in this study results from the choice of the type of structural analysis that is performed to develop fragility functions. Both static and dynamic procedures are implemented to derive fragility curves from the building's mechanical model.

Firstly, based on the static pushover analysis of the structure, a capacity-spectrum method (Fajfar 1999) is used to estimate the performance point of the structure by comparing the capacity curve and the demand spectrum. A lateral static load is applied to the structure, along its longitudinal direction, to generate the pushover curve. The latter is then converted into an acceleration-displacement response spectrum (ADRS) by using the first-mode transformation. The determination of the performance point is carried out with an iterative process that uses inelastic demand spectra with ductility-based reduction factors (Fajfar 1999). In this study, response spectra from natural strong-motion records are used to account for the variability in earthquake shaking. A set of 200 records are selected and applied with the capacity-spectrum approach, resulting in the generation of 200 performance points for each capacity curve. Ground motions have been selected from various databases (Ambraseys et al. 2004, PEER 2011) and they have been chosen so as to span a wide range of ground-motion characteristics, such as amplitude, frequency content and duration. An automated procedure to determine the performance point from unsmoothed de-

mand spectra has been used, which is adapted from the CAsP (Capacity Assessment Program) procedure developed by Rossetto and Elnashai (2005). Finally, the coordinates of the performance points (i.e. spectral displacement and acceleration) are converted back into inter-story drift and spectral acceleration at the first mode (i.e. at $T_1 = 0.33$ s). A simple regression procedure is then performed on the ‘cloud’ of points (Cornell et al. 2002) to obtain the fragility curve parameters for each model.

In addition, a series of non-linear time-history analyses are also performed on each model. The same set of ground motions as in the static analysis is used. Accelerograms are applied at the base of the structure, along the longitudinal direction. Maximum transient inter-story drifts are then used to represent the structural response for each applied accelerogram. Similarly to the static procedure, a regression is performed on the pairs $[SA(T_1 = 0.33 \text{ s}), \text{drift}]$, resulting in the estimation of the median and the standard deviation of the associated fragility curves.

Table 3 displays the fragility parameters for each of the three structural models and each of the analysis procedures (i.e. static and dynamic). For now, the variability in the mechanical properties is not accounted for and only the original deterministic values from Table 1 are used for each model. A good agreement is found between the fragility parameters obtained from static pushover procedure and time-history analyses, even though the static procedure has a tendency to overestimate the ‘yield’ damage probability and underestimate the probability of ‘collapse’ state, when compared to the results from dynamic analysis. These differences may be caused by the bilinearisation of the pushover curves, which has a tendency to attenuate the effects of the peaks (i.e. corresponding to the failure of infill walls, see Figure 2). Therefore, the global strength of the building may be underestimated in the elastic range (i.e. until d_y is reached), while the bilinear curve induces a steady plateau up to d_u , which is not the case in the actual pushover curve. Moreover, the sudden strength reduction due to the failure of infill walls might induce a global failure of the building under dynamic loading and this phenomenon is not accounted for in the static pushover analysis. A slight underestimation in the prediction of collapse state by the static pushover analysis has also been observed by Mwafy and Elnashai (2000) in their analysis of a group of RC structures. Finally, the standard deviation of the fragility curves is also greater when using the capacity spectrum approach. This might result from the use of unsmoothed response spectra during the estimation of performance points because the curves are jagged in ADRS space and the accuracy of the determination of the intersection with the capacity curve is consequently affected.

Table 3: Parameters of the fragility curves for the various configurations, using $SA(T_1)$ expressed in m/s^2 as the intensity measure. α and β are the mean and standard deviation of the lognormal distribution, respectively.

Model	Procedure	Yield		Collapse	
		α_y	β_y	α_c	β_c
1	static	3.42	0.65	18.48	0.65
	dynamic	4.17	0.52	15.35	0.52
2	static	3.59	0.67	20.30	0.67
	dynamic	4.33	0.51	16.55	0.51
3	static	3.49	0.58	18.34	0.58
	dynamic	4.34	0.51	16.63	0.51

4 SENSITIVITY ANALYSIS

The objective of this section is to rank in terms of importance the different sources of epistemic uncertainty, namely the four mechanical parameters, the type of structural model and the analysis procedure (static or dynamic), as described in section 3. A efficient technique can rely on variance-based sensitivity global analysis (GSA), which can provide the main and the total effects (defined using the Sobol’ indices) associated to each source of uncertainty (Saltelli et al. 2008, among others). In this approach, the epistemic uncertainty associated to the choice of the structural model and the type of procedure is accounted for by assigning an indicator (denoted \mathbf{C}), i.e. a discrete random variable taking two or three integer values, namely $\{1, 2, 3\}$ and $\{1, 2\}$ for the structural model and the procedure, respectively. The estimation of the Sobol’ indices can be conducted using different algorithms, like the Monte-Carlo-based Sobol’ algorithm (Saltelli 2002). See Saltelli et al. (2008) for a more complete review and a full mathematical description.

4.1 Meta-modeling strategy

On the other hand, GSA requires a large number of model evaluations (of the order of thousands), which is hardly applicable for long-running numerical codes. In the present study, one single simulation requires around half an hour to run. This problem can be solved by using meta-modeling techniques (Storlie et al. 2009, among others), consisting in replacing the numerical model by a mathematical approximation referred to as a ‘meta-model’ (also named ‘response surface’, or ‘surrogate model’). These approximations are characterized by short run times and hence can be run many times.

We, therefore, propose to construct a meta-model approximating the model output as a costless-to-evaluate function of the four continuous input mechanical variables. In this view, 40 learning samples were randomly selected (within the admissible bounds of each of the four mechanical parameters, see Table 2) using a Latin hypercube design (McKay et al. 1979) in combination with the ‘maxi-min’ space-filling design criterion (Koehler and Owen 1996). For each of these combinations, the four different outputs are evaluated (using a com-

puter grid architecture of 64 CPUs). Several types of meta-models exist, e.g.: simple polynomial regression techniques, non-parametric regression techniques, kriging modeling and artificial neural networks. Because of the high non-linearity of the numerical model, we used the recently-developed ‘Adaptive Component Selection and Shrinkage Operator’ surface-approximation procedure (Storlie et al. 2010). The approximation quality is assessed based on the coefficient of determination using the package CompModSA (<http://cran.r-project.org>) of the R software (<http://www.R-project.org/>). The afore-described procedure is conducted for each of the $3 \times 2 = 6$ combinations of different types of models and procedures and for four model outputs, namely the two median values and the two standard deviations (α_y , β_y , α_c and β_c). In total, $6 \times 4 = 24$ meta-models were constructed, each of them reaching a high (greater than 94%) coefficient of determination.

4.2 Computation of the main and total effects

We calculated the main and total effects using the Monte-Carlo algorithm of Saltelli (2002). Depending on the values of both indicators of the structural model and the analysis procedure, a different meta-model among the 24 is selected to evaluate the sensitivity indices. Main effects represent the first-order contributions of each parameter, without accounting for interaction terms, and they are generally used to rank the influence of the different sources of uncertainties. Total effects, on the other hand, include the contribution of the interaction terms (e.g. the mixed contribution of two or more different parameters) and they can be used to evaluate the complexity of the model.

Figure 3 presents the results using 20 000 Monte-Carlo samples. Note that preliminary convergence tests showed that this number of Monte-Carlo samples gives satisfactory convergence. Several observations can be made:

- using the main effects as a measure for uncertainty ranking (Saltelli et al. 2008), we show that the type of analysis procedure (static or dynamic) influences the most (with main effect exceeding 50%) α_y , whereas all sources of uncertainty appear at approximately the same level for α_c (below 20%);
- using the total effects as a way of identifying negligible parameters (Saltelli et al. 2008), we show that no sources of uncertainty can be neglected considering both α_y and α_c (given that the total effects all exceed 10%);
- the type of analysis procedure (static or dynamic) influences the most (with a main effect exceeding 80%) both β_y and β_c ;

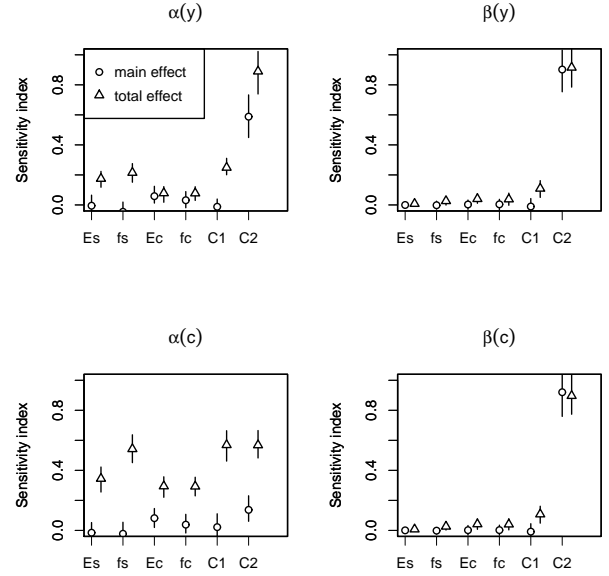


Figure 3: Main (dots) and total (triangles) effects associated to the four mechanical parameters (E_s , f_s , E_c and f_c) and the two types of criteria (C1 and C2) for the four outputs. The error bars correspond to the confidence intervals calculated using a bootstrap procedure. See text for more details.

- given the low values of the total effects ($< 1 - 2\%$), the four mechanical parameters can be fixed at their nominal values considering both β_y and β_c ;
- the differences between main and total effects on α_c (the dot and triangle-type markers) highlight the presence of high interactions between the input parameters (in particular regarding f_s and both types of model).

5 DISCUSSION

As shown by Figure 3, the global variability in the fragility models is mainly explained by the type of analysis procedure (i.e. criterion C2). This observation is corroborated by the fragility parameters in Table 3, where the differences between parameters from static and dynamic analyses are greater than the ones observed between the structural models. Since the effects from the variability of the other parameters appear to be overpowered by the criterion C2, it has been decided to compute first-order Sobol’ indices (i.e. the main effects) for each of the analysis procedures taken separately (see Figure 4).

It can be observed on Figure 4 that the main effects of the different parameters are very low when the static procedure is used (i.e. the rest of the effects I, representing the interaction terms, is high, around 70%). Conversely, in the case of the dynamic analyses, main effects of some parameters are more significant (i.e. more than 20%) and the role of the interactions seems to be reduced (i.e. lower values for I). One of the possible interpretations of these results could

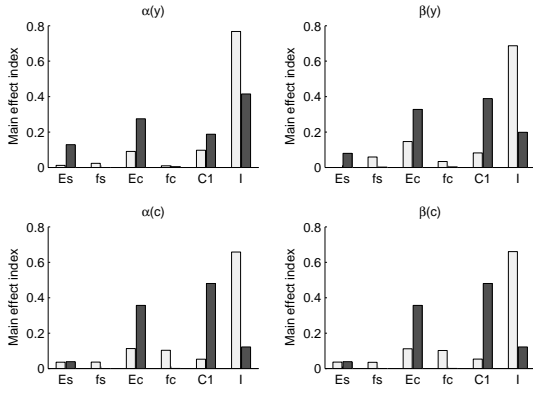


Figure 4: Main effects associated to the four mechanical parameters (E_s , f_s , E_c and f_c) and the type of structural models (C1) when the capacity curve approach (light gray bars) and the dynamic analyses procedure (dark bars) are considered separately. I represents the effects due to interactions between the five criteria; they are not explained by the sole consideration of main effects.

be that a dynamic procedure might be able to better represent the contribution of the uncertain parameters through first-order approximations; whereas, in the case of a static procedure, the role of each parameter taken individually is not clearly translated into the final results, therefore requiring the use of interaction terms to build a sound model. One has to note also that the main effects of E_c and C1 are the highest, which means that the variability of the Young's modulus for concrete and in the choice of the structural model are mainly influencing the structural response in this specific case. The effect of the type of structural models is even more visible when the structure is in the nonlinear range, i.e. for the fragility parameters for the 'near-collapse/collapse' damage state, which is in agreement with the assumptions made in Section 3.2.

These results on fragility parameters can also be propagated to scenario-based damage estimates, which are easier to understand by local planners in terms of uncertainties in losses, for instance. To show the discrepancies induced by the different uncertainties, the 40 learning samples from the mechanical parameters analysis have been used to plot numerous combinations of fragility curves (i.e. 40×3 structural models $\times 2$ analysis procedures $\times 2$ damage states, giving 480 curves), which are represented in Figure 5. This allows for a better visualization of the effects on the parameters of the fragility curves (α and β). The derived curves seem to be well constrained, especially for the yield damage state, despite all the uncertainties that were introduced.

Based on the series of curves from Figure 5, some hypothetical scenarios are carried out, by considering a constant hazard level over an area containing 100 buildings of the type studied here. There is no physical reality behind this scenario, as the aim is only to demonstrate the implications of uncertainties in a fragility function on the results of a given damage assessment. Three arbitrary hazard levels are selected [$SA(T_1)$ equal to 2.5, 10 and 20 m/s^2], to evaluate the

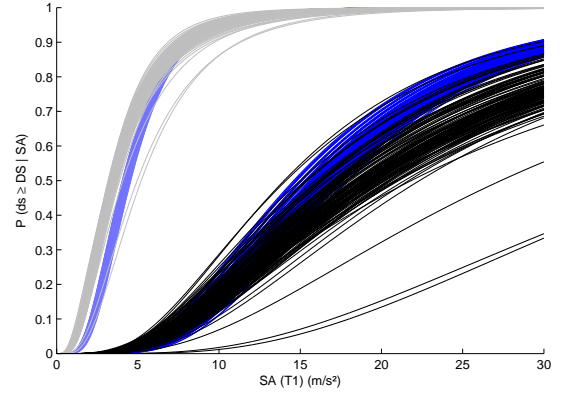


Figure 5: Series of fragility curves plotted for the different combinations of mechanical parameters (i.e. the 40 learning samples) and structural models, for the two types of analyses (i.e. blue for dynamic and gray/black for static). The yield damage state corresponds to the light blue and gray lines, and the collapse state to the dark blue and black lines.

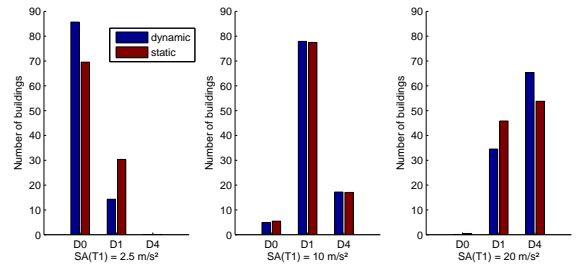


Figure 6: Damage distribution for a hundred buildings submitted to different constant hazard levels, with D0 corresponding to the intact state, and D1 and D4 to 'yield' and 'near-collapse/collapse', respectively.

resulting damage at various positions of both fragility curves (i.e. around the median and at the extremities of the distribution).

The damage distributions shown in Figure 6, resulting from the series of fragility functions computed earlier, confirms that both types of analytical procedures tend to give similar results. Results are, for example, almost identical for $SA(T_1) = 10 \text{ m/s}^2$ because this value corresponds to a position where the fragility curves from both types of analyses are almost overlapping (see Figure 5). On the other hand, the discrepancies are more visible when the extremities of the distributions are solicited, due to the increasing influence of the fragility parameter β . This effect has most consequences at the lower ends of the distribution (i.e. weak shaking), where the relative gap between small probability values can induce large differences when many buildings are assessed in the context of an urban risk scenario. For instance, for $SA(T_1) = 2.5 \text{ m/s}^2$, the damage distribution based on the static pushover approach estimates around 30 buildings in the D1 damage state, whereas the one that is based on dynamic analyses suggests that only around 15 will be in this state. Even if one may argue that the order of magnitude is comparable, this two-to-one ratio may still be a source of large inaccuracies when global scenario-based losses are assessed at a regional or urban scale.

6 CONCLUSIONS

In this study, we have presented an analysis of the uncertainties associated with the derivation of fragility curves for mid-story pre-code RC buildings, which are common in many parts of the world. We considered three sets of uncertainties: the material properties, the overall structural behavior and the analysis type. A state-of-the-art sensitivity analysis is conducted using a series of meta-models (developed to make the required computations tractable) to understand the influence of the different choices and their interactions on the parameters of the lognormal fragility curves. It is concluded that the analysis type (capacity spectrum approach or nonlinear time-history analysis) has the largest impact on the fragility curves and the influence of the other choices is minimal. This choice can lead to a factor of two difference in the estimated number of damaged buildings for certain scenarios. The approach used for this analysis (Sobol' indices) is a powerful technique for uncertainty analyses and it is recommended that it is applied for other structural types and other uncertain parameters to study whether the conclusions reached here are generally applicable. The hazard component has been left out of the present studies but future plans should include the sources of uncertainties associated with the hazard intensity estimation, so that all components within the risk assessment procedure can be compared in the context of a seismic scenario.

REFERENCES

- Ambraseys, N., P. Smit, J. Douglas, B. Margaris, R. Sigbjörnsson, S. Olafsson, & P. Suhadolc (2004). Internet site for European strong-motion data. *Bollettino di Geofisica Teorica e Applicata* 45, 113–129.
- ASCE (2007). *Seismic rehabilitation of buildings (ASCE-46)*. American Society of Civil Engineers.
- Cornell, C., F. Jalayer, R. Hamburger, & D. Foutch (2002). Probabilistic basis for 2000 SAC Federal Emergency Management Agency steel moment frame guidelines. *Journal of Structural Engineering* 128, 526–533.
- Crowley, H., M. Colombi, V. Silva, N. Ahmad, M. Fardis, G. Tsionis, A. Papaïlia, F. Taucer, U. Hancilar, & A. Yakut (2011). Fragility functions for common RC building types in Europe. Technical report, Systemic Seismic Vulnerability and Risk Analysis for Buildings, Lifeline Networks and Infrastructures Safety Gain (SYNER-G), Project of the EC Framework Programme 7.
- Eurocode 2 (2005). *Calcul des structures en béton NF EN 1992-1-1*. AFNOR.
- Fajfar, P. (1999). Capacity spectrum method based on inelastic demand spectra. *Earthquake Engineering and Structural Dynamics* 28, 979–993.
- Gehl, P., D. Seyedi, & J. Douglas (2013). Vector-valued fragility functions for seismic risk evaluation. *Bulletin of Earthquake Engineering* 11. In press.
- Grünthal, G. (1998). European macroseismic scale 1998 (EMS-98). Technical report, Cahier du Centre Européen de Géodynamique et de Séismologie, Luxembourg.
- Jalayer, F., I. Iervolino, & G. Manfredi (2010). Structural modeling uncertainties and their influence on seismic assessment of existing RC structures. *Structural Safety* 32, 220–228.
- Kent, D. & R. Park (1971). Flexural members with confined concrete. *Journal of the Structural Division* 97, 1969–1990.
- Koehler, J. & A. Owen (1996). *Computer experiment*. In: Ghosh, S., Rao, C.R. (Eds.), *Handbook of Statistics*. New-York, USA: Elsevier Science.
- Kwon, O. & A. Elnashai (2007). The effect of material and ground-motion uncertainty on the seismic vulnerability curves of rc structures. *Engineering Structures* 28, 289–303.
- McKay, M., R. Beckman, & W. Conover (1979). A comparison of three methods for selecting values of input variables in the analysis of output from a computer code. *Technometrics* 10, 239–245.
- Milutinovic, Z. & G. Trendafiloski (2003). WP4 vulnerability of current buildings. tech rep, Risk-UE: An advanced approach to earthquake risk scenarios with applications to different European towns. Technical report, Risk-UE project.
- Mwafy, A. & A. Elnashai (2000). Static pushover versus dynamic collapse analysis of RC buildings. *Engineering Structures* 23, 407–424.
- Negulescu, C., K. Wijesundara, & E. Foesrter (2013). Seismic damage assessment of regular gravity design buildings. *Engineering Structures*. Submitted.
- Pagnini, L., R. Vicente, S. Lagomarsino, & H. Varum (2011). A mechanical model for the seismic vulnerability assessment of old masonry buildings. *Earthquakes and Structures* 2, 25–42.
- PEER (2011). Users manual for the PEER ground motion database web application. Technical report, Pacific Earthquake Engineering Research Center.
- Rossetto, T. & A. Elnashai (2005). A new analytical procedure for the derivation of displacement-based vulnerability curves for populations of RC structures. *Engineering Structures* 27, 397–409.
- Rota, M., A. Penna, & G. Magenes (2010). A methodology for deriving analytical fragility curves for masonry buildings based on stochastic nonlinear analyses. *Engineering Structures* 32, 1312–1323.
- Saltelli, A. (2002). Making best use of model evaluations to compute sensitivity indices. *Computer Physics Communications* 145, 280–297.
- Saltelli, A., M. Ratto, T. Andres, F. Campolongo, J. Cariboni, D. Gatelli, M. Saisana, & S. Tarantola (2008). *Global sensitivity analysis: The Primer*. Chichester, UK: Wiley.
- Sousa, R., T. Eroglu, D. Kazantzidou, M. Kohrangi, L. Sousa, R. Nascimbene, & R. Pinho (2012). Effects of different modelling assumptions on the seismic response of rc structures. *Proceedings of the Fifteenth World Conference of Earthquake Engineering, Lisbon, Portugal*.
- Storlie, C., H. Bondell, B. Reich, & H. Zhang (2010). Surface estimation, variable selection, and the non parametric oracle property. *Statistica Sinica* 21, 679–705.
- Storlie, C., L. Swiler, J. Helton, & C. Sallaberry (2009). Implementation and evaluation of nonparametric regression procedures for sensitivity analysis of computationally demanding models. *Reliability Engineering and System Safety* 94, 1735–1763.
- Zentner, I. (2011). Méthodes numériques pour l'évaluation de la fragilité sismique. application à la maquette du benchmark SMART. *Proceedings of AFPS 2011, Ecole des Ponts Paris-Tech, Paris*, 1139–1148.